RSC Advances

ROYAL SOCIETY OF CHEMISTRY

www.rsc.org/advances

Journal Name

RSCPublishing

ARTICLE

Surfactant-free Hydrothermal Synthesis of Cu_2ZnSnS_4 (CZTS) Nanocrystals and Photocatalytic Properties

Cite this: DOI: 10.1039/xoxxoooooox

Jing Wang, Peng Zhang*, Xuefeng Song, and Lian Gao*

Received ooth January 2012,
Accepted ooth January 2012

DOI: 10.1039/xoxxoooooox

www.rsc.org/

As a low cost and environment-friendly solar absorber material, Cu_2ZnSnS_4 (CZTS) has aroused great interest in both photovoltaic and photocatalytic applications. The development of low temperature and green chemical route for preparation of this quaternary sulfide compound still remains a challenge. We present here a surfactant-free hydrothermal method for the preparation of CZTS nanocrystals with an average size of 12 nm and photoactivity in hydrogen production. Ammonia was proposed to play a key role in confining the particle sizes. The properties of the CZTS nanoparticles were characterized using XRD, Raman, XPS, TEM, and UV-vis absorption. The photocatalytic properties of the as-synthesized CZTS nanoparticles were tested both in thin films and in slurry systems.

Introduction

Research on high-efficient and low-cost solar absorber materials has attracted continuous attention due to the increasing concerns in both energy and environments.[1-4] $Cu(InGa)Se_2$ (CIGS) has become one of the representative materials for sustainable high-efficiency solar cells and its energy conversion efficiency has achieved 19.9%.[5-7] Due to the scarcity and the high cost of In and Ga elements in CIGS, alternative candidate materials are also under intense investigation. CZTS, having analogue crystal structure to CIGS, has attracted much attention due to its high absorption coefficient of over 10^4 cm^{-1}, optimal band gap of approximately 1.5 eV, natural abundance, and environmental friendliness.[8-15] Katagiri *et al.*[16] have prepared CZTS solar cells with a conversion efficiency of 6.7% by sputtering and vapor deposition. Recently, the efficiency of $Cu_2ZnSn(Se,S)_4$ solar cells has been further increased to 12.0% after optical-designing.[17] The direct applications of CZTS in photoelectrochemical (PEC) and photochemical reaction have been recently investigated. Yokoyama *et al.*[18] reported a solar-to-H_2 conversion efficiency of 1.2% for the first time on co-sputtered CZTS thin films with the structure of $Pt/TiO_2/CdS/CZTS/Mo$. The stability of CZTS thin films in PEC reaction has been improved by surface modification with CdS and TiO_2 layers through spin coating method.[19] Recently, CZTS powders were applied in reduction of water to hydrogen, and the efficiency was enhanced significantly by modifying the CZTS via novel Au/CZTS core/shell NPs.[20]

Conventional CZTS thin films with high conversion efficiency are generally prepared by directly depositing CZTS on substrates into thin films or electrodes using physical method at high temperature in vacuum. In order to decrease the cost of material preparation, various non-vacuum methods have been adopted for the synthesis of CZTS nanocrystals and thin films. Hot-injection solution synthesis,[21] sol-gel method,[22] ture solution,[23] electrochemical deposition,[24] spray and sputter deposition,[25] and successive ionic layer absorption and reaction (SILAR) technique have been reported.[26] However, most techniques require expensive instruments, harsh conditions or application of long chain surfactants. Hydrothermal and solvothermal methods have been widely used for preparation of CZTS nanowires, sphere-like and hierarchical particles at relatively low temperature.[12,15,27,28] However, surfactants, *e.g.* polyvinylpyrrolidone (PVP) and oleylamine (OA), is still often utilized to control the particle sizes and/or morphologies. The surface adsorption of surfactants to some extent hindered the electron transfer among particles when applied as photovoltaic or photoelectrocatalytic thin films. The use of surfactants also introduces environmental issues when scaled up in industry. In this regard, the surfactant free synthetic method, a green process, is desired.

Herein, we adopted an ammonia-assisted hydrothermal method without usage of surfactants or toxic reductants such as hydrazine for preparation of CZTS nanocrystals. The formation mechanism and photocatalitic activity of the CZTS samples are addressed.

Experimental Section

Synthesis of CZTS Nanocrystals: Copper(II) acetate ($Cu(Ac)_2$), zinc acetate ($Zn(Ac)_2$), tin(II) chloride ($SnCl_2$), thioacetamide (TAA), europium nitrate ($Eu(NO_3)_3•6H_2O$), sodium sulfide (Na_2S) and sodium sulfite (Na_2SO_3) were purchased from Aladdin and used without further purification. Copper acetate (10 mL, 0.2 mol L^{-1}), zinc acetate (10 mL, 0.1 mol L^{-1}), tin dichloride (10 mL, 0.1 mol L^{-1}), and thioacetamide (20 mL, 0.2 mol L^{-1}) solutions were prepared using miliQ water, keeping the stoichiometry of Cu:Zn:Sn:S as 2:1:1:4. Subsequently, an ammonia solution was added to adjust the pH ≈ 7 with constant magnetic stirring for several minutes. The whole process was protected with nitrogen. The mixture was then

transferred to a Teflon-lined stainless steel autoclave of 100 ml capacity. The autoclave was sealed and held at 200 ^{o}C for 24 h. The resulting product was centrifuged and washed with miliQ water and ethanol for three times. Finally, the as-synthesized nanocrystals were dried at 60 ^{o}C. Control samples were prepared by using NaOH instead of ammonia to adjust the pH values, by reducing 50% of TAA in the synthesis, and by synthesis without adding ammonia, respectively.

Characterization of photocatalysts: The crystallographic structures of the as-synthesized products were identified by X-ray diffraction (XRD, Ultima IV, Rigaku Co., LTD, Japan Cu Kα, λ = 1.54178 Å) and Raman spectrometer (Bruker Optics Senterra R200-L). Transmission electron microscopy (TEM) images of the as-obtained products were performed on JEM-2010HT Analytical transmission electron microscope operated at an acceleration voltage of 200 KV. Scanning electron microscope (SEM) images of the as-obtained products were performed on NOVA Nano SEM 230. Energy-dispersive X-ray spectra were obtained by energy-dispersive X-ray spectroscopy (EDS) on JSM7600F. The chemical binding energy of the products was examined on a Kratos AXIS Ultra DLD spectrometer. UV-vis absorption was carried out by UV-vis spectroscopy (EV300). Nitrogen absorption and desorption measurement was performed on Quantachrome Autosorb IQ. The surface area was calculated by the Brunauer-Emmett-Teller (BET) method.

Photocatalytic Characterization: The photocatalytic properties of CZTS nanoparticles were tested by pasting the powders on Fluorine-doped Tin Oxide (FTO) substrates as photoelectrode through a doctor blade method followed by annealing in Ar at 380 ^{o}C. The photoelectrochemical (PEC) measurements were performed by a three-electrode experimental setup (CHI660D electrochemical workstation, Chenhua, Shanghai). A platinum wire and a saturated calomel electrode (SCE) acted as the counter and reference electrode, respectively. A Xenon lamp (300 W, Newport 6258, USA) with 400 nm cutoff was used as a light source through a fiber optic lightguide. The light intensity was 13 mW/cm^{-2} measured by an irradiatometer. The photocurrents of the thin films were measured in 0.1 mol L^{-1} $Eu(NO_3)_3$•$6H_2O$ aqueous solution. Photocatalytic reactions of the slurry system were carried out in a gastight quartz tube with side-irradiation using a 500-W Xenon lamp as a light source. CZTS power (25 mg) was dispersed into aqueous solution (25 ml) by a magnetic stirrer. Na_2SO_3 (0.25M)/Na_2S (0.35M) was used as sacrifice agents in this reaction to scavenge the photo-generated holes. Nitrogen was bubbled through the solution to remove the dissolved oxygen before photocatalytic reactions. Pt nanoparticles were photo-deposited in situ as co-catalyst on CZTS particles using different amounts of $K_2PtCl_6 \cdot H_2O$ in Na_2SO_3/Na_2S solution. The amount of hydrogen evolved was detected using gas chromatography (GC7900, Tianmei, China) by syringe injection. Comparison experiments showed no hydrogen evolution in the dark.

Results and Discussion

X-ray diffraction (XRD) pattern of the as-synthesized nanoparticles is shown in Fig. 1. The diffraction peaks of CZTS sample at 2θ = 28.5, 33.0, 47.3, 56.2, 59.0, 69.2, and 76.4° can be assigned to the diffraction of (112), (200), (220), (312), (224), (008), and (332) planes of the kesterite CZTS (JCPDS, Card, no.26-0575), respectively. The average crystallite size calculated using Debye-Scherrer analysing based on the full width at half maximum (FWHM) of (112) diffraction peak is 12 nm. The diffraction pattern shows well crystallized nanoparticles with no apparent trace of secondary phase. Raman spectrum of the nanoparticles, Fig. 2, further supports the formation of CZTS structure. The intensive scattering at 285 cm^{-1}, 334 cm^{-1}, and 361 cm^{-1} are representative for CZTS and close to the literature values.[29] The absence of peaks at 278 cm^{-1}, 351 cm^{-1} and 295-303 cm^{-1}, 355 cm^{-1} suggests the absence of ZnS and Cu_2SnS_3 in the sample.[29]

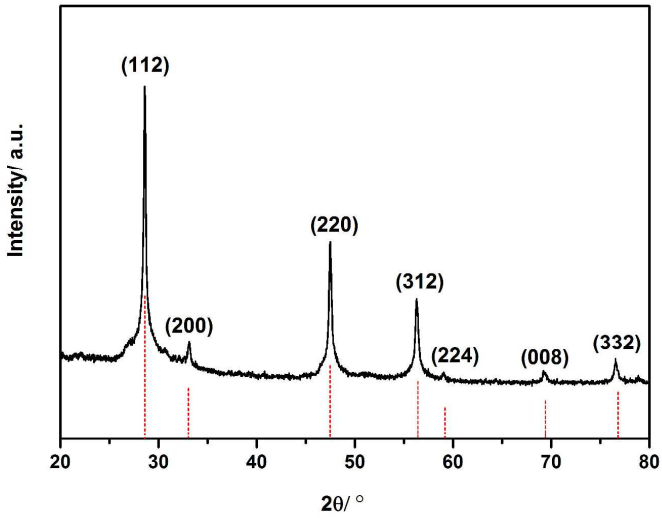

Fig. 1 XRD pattern of as-synthesized nanoparticles. The fine line shows the simulated pattern of kesterite CZTS (JCPDS no. 26-0575).

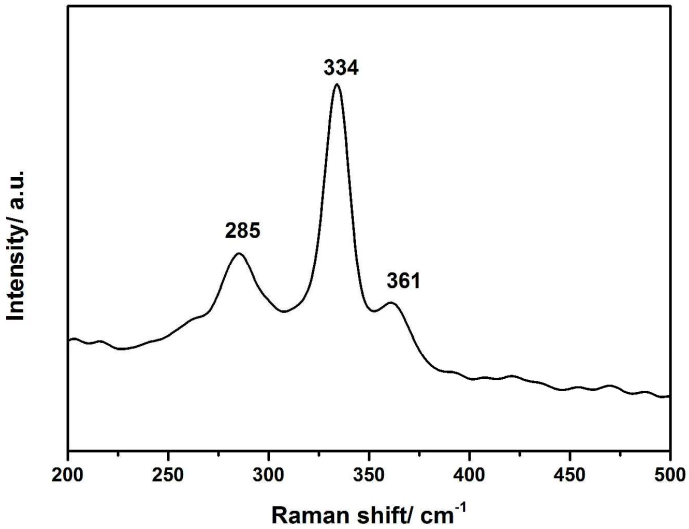

Fig. 2 Raman spectrum of CZTS nanoparticles. The manly peaks are 334, 285, 361cm^{-1}.

Journal Name

RSCPublishing

ARTICLE

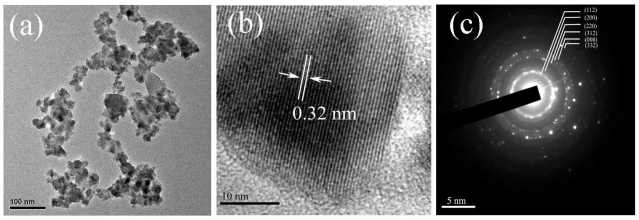

Fig. 3 (a) TEM image, (b) HRTEM image, and (c) SAED rings of CZTS nanoparticles.

The morphology of the nanoparticles is observed from TEM image, Fig. 3a, which shows faceted nanoparticles with size ranging from 2 to 30 nm. The well crystallized nature of the nanoparticles based on their XRD patterns is consistent with the high resolution TEM (HR-TEM) image, Fig. 3(b), which shows clear lattice fringes with interplanar distance of 0.32 nm, corresponding to the (112) facets. The selected area electron diffraction (SAED) pattern in Fig. 3(c) matches the polycrystalline structure of CZTS. The diffraction rings correspond to the (112), (200), (220), (312), (008), and (332) planes, respectively.

The surface area measured through nitrogen adsorption-desorption isotherm is 133.54 m^2 g^{-1}, which corresponds to a particle size of 16 nm assuming a spherical morphology. This is consistent with the results from XRD and TEM. The nitrogen adsorption-desorption isotherm for the as-synthesized CZTS is typical type IV with a H_3 hysteresis loop at high relative pressure (P/P_0>0.5) (Fig. S1).

Table 1. Five representative EDX data taken from CZTS nanoparticles.

Element	Atomic % of 5 different locations on nanoparticles					Atomic ratio
Cu	23.08	23.35	22.32	22.33	26.53	1.96
Zn	12.50	15.07	13.70	11.61	15.73	1.14
Sn	11.90	11.50	12.14	12.85	11.74	1.00
S	52.53	50.08	51.84	53.21	46.01	4.22

The elemental stoichiometry of CZTS nanoparticles, determined through (EDS) analysis on five investigated spots, shows the atomic ratio of Cu: Zn: Sn: S of 1.96: 1.14: 1.00: 4.22, as shown in Table 1. This is close to the ideal ratio of 2: 1: 1: 4. The metal ratio is also close to the stoichiometric ratio of the metal precursors. The oxidation states of the constituent elements were also determined using X-ray photoelectron spectroscopy (XPS) spectra of Cu 2p, Zn 2p, Sn 3d, and S 2p core levels, Fig. 4. The peaks at 1021.8 eV and 1044.9 eV of Zn 2p, splitted by 23.0 eV, suggest the status of Zn (II). The doublet peaks of copper locate at 932.0 eV (Cu 2p3/2) and 951.0 eV (Cu 2p1/2), respectively. The peak separation of 19.8 eV that is close to the standard 19.9 eV indicates the oxidation state of Cu(I). Sn (IV) is confirmed by the 8.7 eV separation of Sn 3d peaks, observed at 486.4 eV and 495.1 eV, respectively. The S 2p spectrum shows two peaks at 161.5 and 162.7 eV with a separation of 1.2 eV, which are close to those reported for S in sulfide phases.[8-15,30,31] Therefore, both the stoichiometry and the oxidation status of the elements suggest the formation of quaternary compound. The absence of N peaks in the survey scan spectrum (Fig. 4e) indicates the absence of ammonia residue on CZTS particle surfaces.

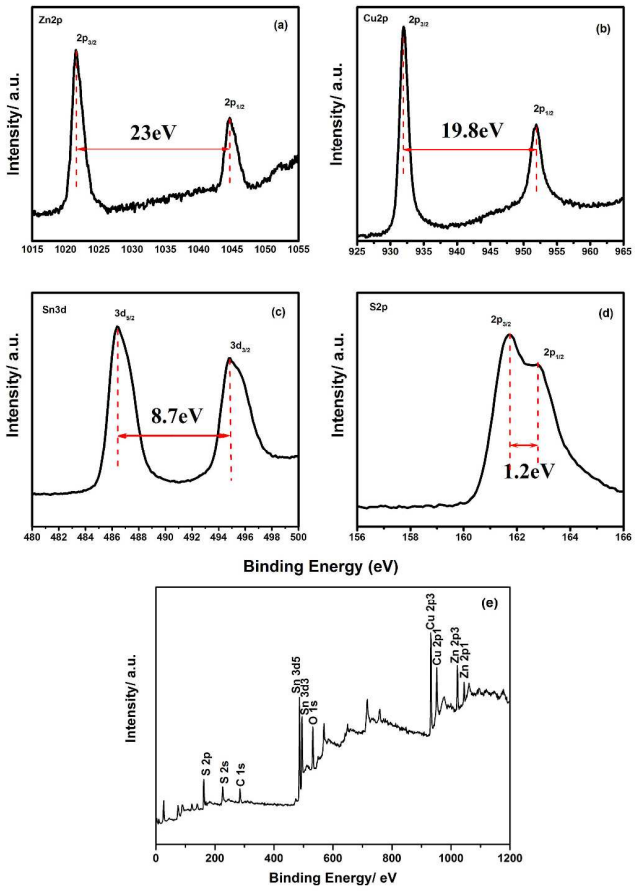

Fig. 4 XPS analysis of CZTS nanoparticles; (a) Zn 2p, (b) Cu 2p, (c) Sn 3d, (d) S 2p core levels, and (e) survey scan, respectively.

The UV-vis absorption spectrum of the CZTS nanoparticles is shown in Fig. 5. The direct band gap of CZTS is obtained by a linear extrapolation of a plot of $(\alpha h\nu)^2$ versus energy, where α and

hν represent the absorption coefficient and the photon energy, respectively. The direct optical band gap of CZTS is calculated to be 1.52 eV, which is consistent with the literature value.[8-15] This also confirms the absence of ZnS and Cu_2SnS_3, whose band gaps are 3.7 and 0.93 eV, respectively.[32,33]

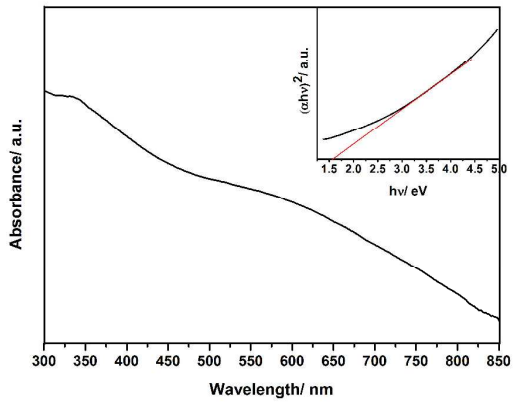

Fig. 5 UV-vis absorption spectrum of the CZTS nanoparticles. Inset shows the plot of $(\alpha h\nu)^2$ vs photon energy.

The chemistry of the hydrothermal synthesis of the quaternary sulfide nanocrystals is related to the coordination between the ammonia molecules and the metal ions, as well as the slow dissociation of sulfide precursor. Upon dissolution of copper, zinc, and tin salts, Cu^{2+} ions are reduced into Cu^{+} by tin (II) (1), which is accompanied with color change of the solution from blue to pale green. The dissociation of thioacetamide into sulfide ions (S^{2-}) under hydrothermal condition is ascribable to the steps (2)-(6).[26] In acidic medium, protanation (the pH value of precursors is ~ 3.8) of thioacetamide produces intermediate product (3), which further dissociates into H_2S (4). In aqueous medium, H_2S dissociates into HS^- and S^{2-} (5,6).

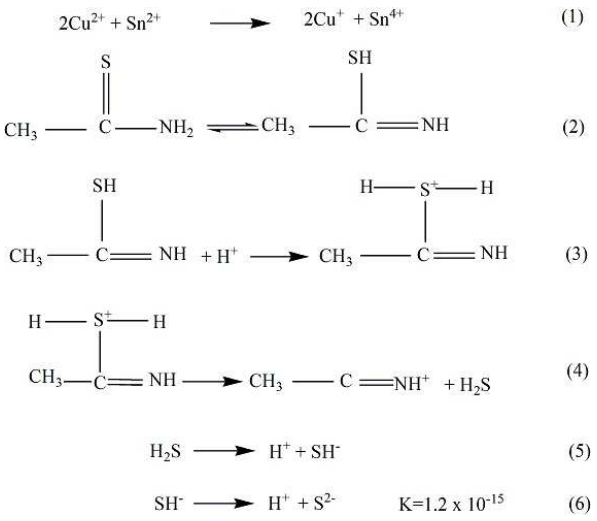

We propose that ammonia plays a crucial role in the synthesis of nanocrystals.[34,35] The basic nature of the ammonia adjusts the dissociation of thioacetamide (TAA) and the release of sulfide ions as in the steps (5) and (6). The reaction between the free metallic ions and S^{2-} initiates the nucleation of CZTS. Due to the strong coordination between ammonia molecules and Cu^{2+} and Zn^{2+}, the decoordination of the metal ions from ammonia is thermodynamically unfavoured. The concentration of the free metal ions (without coordination with ammonia) is thus kept at a low level due to the equilibrium between the free ions and the coordinated ones. In addition, the slow release of S^{2-} from TAA precursor further constrains the growth of CZTS crystals, which finally results in ultra-fine particles. When the amount of TAA is reduced to 50%, the obtained particle size is remarkably decreased (Fig. S2d) yet secondary phases appear (Fig. S3c). During the synthetic process, ammonia molecules might still be adsorbed on the surface of the nucleated CZTS nanocrystals through coordination bonds with the surface metal atoms, which lowers their surface energy and hinders the ripening of nanocrystals. Without the use of ammonia, the obtained particles show more aggregation, as shown in Fig. S2. Therefore, ammonia behaves like surfactants during the synthesis process in the solution, which limits the growth and ripening of the crystals and results in nanoparticles without the use of organic surfactants. However, the size confinement effect of ammonia on nanoparticles is still not comparable to the real carbohydrate surfactants. Therefore, we still observe aggregation among the as-prepared than nanoparticles and the particle size distribution is wider (2-30 nm) than those prepared by hot injection methods using organic ligands, *e.g.* oleylamine. [21] The presence of ammonia not only confines the growth of particles, but helps inhibition of the growth of the secondary phases, such as CuS and ZnS. The control samples with application of NaOH and without NaOH and ammonia show obvious diffractions of CuS and ZnS, Fig. S3. This mechanism is still not clear and awaits further investigation.

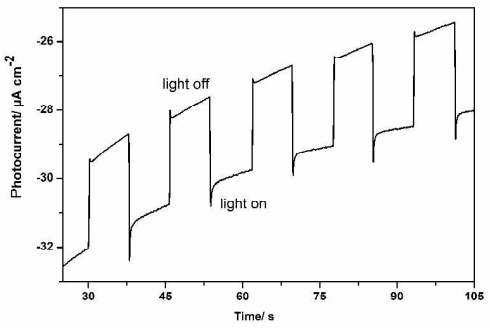

Fig. 6 Chopped photocurrent of CZTS films with a three electrode configuration under a back illumination of 13.8 mW cm^{-2}. The applied bias is 0 V_{SCE}.

The obtained CZTS nanoparticles show p-type photocatalytic property, based on the performance of the thin film made from the powders. Fig. 6 shows the chopped photocurrent of CZTS thin film at an applied bias of 0 V_{SCE}. A cathodic photocurrent of 3 uA cm^{-2} was observed under 13 mW cm^{-2} back illumination. The negative photocurrent indicates a p-type conductivity of CZTS

photoelectrode.[36,37] Upon light on and off, relative large photocurrent transients are observed, which is due to the rich surface defects and accumulation of charges.[38] The relatively low photocurrent is related to the procedure in making photoelectrode and the thickness of the thin films. The thickness of the as-synthesized CZTS thin films by doctor blade coating in this case is ~5 μm, far beyond the transport length of the holes (< 1 μm). [39] Therefore, there was almost no detectable photocurrent of the thin films under front illumination because most of the holes generated from the front surface cannot transport through 5 μm to reach the conducting substrate. The nanocrystals and the thin films in our case were both prepared under a relative lower temperature, which indicates a relatively higher level of surface defects and thus a higher opportunity of charge recombination during photocatalytic process. The mesoporous surface feature of the as prepared thin film (Fig. S4) indicates a high surface area and relative large dark current, which is corresponding to the corrosion of CZTS in electrolyte as shown in Fig. 6. The photocurrent of the obtained thin films is still not comparable to the thin films prepared from high temperature process, such as CZTS wafer,[18] which has less surface defects and grain boundaries.

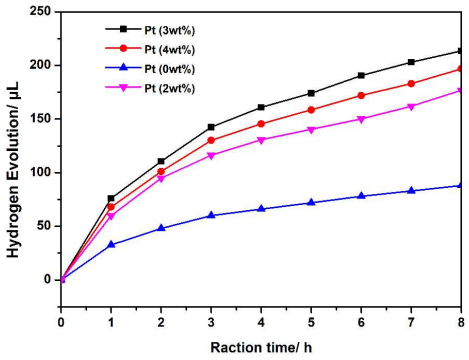

Fig.7 Hydrogen evolution from an aqueous Na_2SO_3 (0.25 mol L^{-1}) and Na_2S (0.35 mol L^{-1}) solution (25 ml) over Pt (0wt%, 2wt%, 3wt%, 4wt%)-loaded CZTS photocatalysts (25 mg); light source, 500-W Xenon lamp, 6.7 mW cm^{-2}; reaction cell, gastight quartz tube with side-irradiation.

The photocatalytic property of CZTS is also confirmed from the solar hydrogen production experiment in slurry system.[40] Fig. 7 shows H_2 evolution of CZTS nanoparticles under a side radiation of a 500 W Xenon lamp in Na_2SO_3 (0.25 mol L^{-1}) and Na_2S (0.35 mol L^{-1}) aqueous solution. The deposition of Pt significantly improves the hydrogen production rate, up to 152.8 uL h^{-1} in the first three hours. The hydrogen production rate varies with the amount of Pt loading. A Pt-loading of 3wt% shows the optimal performance. The hydrogen production rate decreases with illumination time. This is due to the probable photocorrosion of this p-type semiconductor. The Cu(I) is a metastable phase in aqueous solution and S^{2-} is also prone to get oxidized during photocatalytic reaction. However, the observed hydrogen production does show activity of the as synthesized CZTS nanoparticles in photocatalytic reaction.

Conclusions

CZTS nanocrystals were successfully synthesized by an ammonia-assisted hydrothermal method without the usage of any surfactants. Ammonia solution plays an important role in the control over crystal growth, and thioacetamide serves as both sulfur source and reducing agent during the synthesis. The results of XRD, Raman, TEM, EDS, XPS, and UV-vis absorption spectrum verify the kesterite structure of the as-synthesized CZTS with an average size of 12 nm and a bandgap of 1.52 eV. As-synthesized CZTS nanoparticles show photocatalytic activity both in thin films and in slurry systems for hydrogen production in aqueous solution. Further investigation should be performed to improve the photocatalytic performance of CZTS nanoparticles by solving the latent aggregation and photocorrosion issues.

Acknowledgements

The authors greatly acknowledge the financial support by the National Natural Science Foundation of China (No.51172142), Shanghai Municipal Natural Science Foundation (No.12ZR1414300), Starting Foundation for New Teacher of Shanghai Jiao Tong University (No.12X100040119) and the Third Phase of 211 Project for Advanced Materials Science (No. WS3116205006 and WS3116205007).

Notes and references

State Key Lab of Metal Matrix Composites
School of Materials Science and Engineering
Shanghai Jiao Tong University
800 Dongchuan Rd.
Shanghai, P. R. China 200240
E-mail: liangao@mail.sic.ac.cn, pengzhang2010@sjtu.edu.cn

Electronic Supplementary Information (ESI) available: [details of any supplementary information available should be included here]. See DOI: 10.1039/b000000x/

[1] H. Jiang, P. Dai, Z. Feng, W. Fan and J. Zhan, *J. Mater. Chem.,* 2012, **22**, 7502.
[2] M. J. Bierman and S. Jin, *Ener*gy Envi*ron.Sci.*, 2009, **2**, 1050.
[3] V. A. Akhavan, B. W. Goodfellow, M. G. Panthani, C. Steinhagen, T. B. Harvey, C. J. Stolle and B. A. Korgel, *J. Solid State Chem,* 2012, **189**, 2.
[4] Z. Q. Li, J. H. Shi, Q. Q. Liu, Y. W. Chen, Z. Sun, Z. Yang and S. M. Huang, *Nanotechnology,* 2011, **22**, 265615.
[5] K. Woo, Y. Kim and J. Moon, *Energy Environ.Sci.*, 2012, **5**, 5340.
[6] K. Ramasamy, M. A. Malik and P. O'Brien, *Chem. Commun.,* 2012, **48**, 5703.
[7] A. Fischereder, T. Rath, W. Haas, H. Amenitsch, J. R. Albering, D. Meischler, S. Larissegger, M. Edler, R. Saf, F. Hofer and G. Trimmel, *Chem. Mater.,* 2010, **22**, 3399.

[8] K. Hironori, *Thin Solid Films,* 2005, **480–481**, 426.
[9] X. Xin, M. He, W. Han, J. Jung and Z. Lin, *Angew. Chem. Int. Ed.,* 2011, **50**, 11739.
[10] P. Dai, G. Zhang, Y. Chen, H. Jiang, Z. Feng, Z. Lin and J. Zhan, *Chem. Commun.,* 2012, **48**, 3006.
[11] H. Yang, L. A. Jauregui, G. Zhang, Y. P. Chen and Y. Wu, *Nano Lett.,* 2012, **12**, 540.
[12] L. Shi, C. Pei, Y. Xu and Q Li. *J. Am. Chem. Soc.,* 2011, **133**, 10328.
[13] A. Shavel, D. Cadavid, M. Ibáñez, A. Carrete and A. Cabot, *J. Am. Chem. Soc.,* 2012, **134**, 1438 .
[14] C. Zou, L. Zhang, D. Lin, Y. Yang, Q. Li, X. Xu, X. a. Chen and S. Huang, *CrystEngComm*, 2011, **13**, 3310.
[15] Q. Tian, X. Xu, L. Han, M. Tang, R. Zou, Z. Chen, M. Yu, J. Yang and J. Hu, *CrystEngComm,* 2012, **14**, 3847.
[16] H. Katagiri, K. Jimbo, W. S. Maw, K. Oishi, M. Yamazaki, H. Araki and A. Takeuchi, *Thin Solid Films,* 2009, **517**, 2455.
[17] M. T. Winkler, Wang. W, O. Gunawan, H. J. Hovel, T. K. Todorov and D. B. Mitzi, *Energy Environ Sci,* 2014, **7**, 1029.
[18] D. Yokoyama, T. Minegishi, K. Jimbo, T. Hisatomi, G. Ma, M. Katayama, J. Kubota, H. Katagiri and K. Domen, *Appl. Phys. Express,* 2010, **3**, 101202.
[19] J. Wang, P. Zhang, X. Song and L. Gao, *RSC Advances,* 2014, **4**, 21318.
[20] E. Ha, L. Y. S. Lee, J. Wang, F. Li, K. Y. Wong and S. C. E. Tsang, *Adv. Mater.,* 2014, DOI: 10.1002/adma.201400243.
[21] S. C. Riha, B. A. Parkinson and A. L. Prieto, *J. Am. Chem. Soc.,* 2009, **131**, 12054.
[22] K. Tanaka, N. Moritake and H. Uchiki, Sol. *Energy Mater. Sol. Cells,* 2007, **91**, 1199.
[23] G. Wang, W. Zhao, Q. Tian, S. Gao, L. Huang and D. Pan, *ACS Appl. Mater. Interfaces,* 2013, **5**, 10042.
[24] P. Wang, T. Minegishi, G. Ma, K. Takanabe, Y. Satou, S. Maekawa, Y. Kobori, J. Kubota and K. Domen, *J. Am. Chem. Soc.,* 2012, **134**, 2470.
[25] N. M. Shinde, R. J. Deokate and C. D. Lokhande, *J. Anal. Appl. Pyrolysis,* 2013, **100**, 12.
[26] N. M. Shinde, D. P. Dubal, D. S. Dhawale, C. D. Lokhande, J. H. Kim and J. H. Moon, *Mater. Res. Bull.,* 2012, **47**, 302.
[27] Y. L. Zhou, W. H. Zhou, Y. F. Du, M. Li and S. X. Wu, *Mater. Lett.,* 2011, **65**, 1535.
[28] Y. L. Zhou, W. H. Zhou, M. Li, Y. F. Du and S. X. Wu, *J. Phys. Chem. C,* 2011, **115**, 19632.
[29] A. J. Cheng, M. Manno, A. Khare, C. Leighton, S. A. Campbell and E. S. Aydil, *J. Vac. Sci. Technol. A,* 2011, **29**, 051203.
[30] A. Singh, H. Geaney, F. Laffir and K. M. Ryan, *J. Am. Chem. Soc.*, 2012, **134**, 2910.
[31] M. D. Regulacio, C. Ye, S. H. Lim, M. Bosman, E. Ye, S. Chen, Q. H. Xu and M. Y. Han, *Chem. Eur. J.,* 2012, **18**, 3127.
[32] M. Wei, Q. Du, D. Wang, W. Liu, G. Jiang and C. Zhu, *Mater. Lett.,* 2012, **79**, 177.
[33] Y. Wang and H. Gong, *J. Electrochem. Soc.,* 2011, **158**, H800.
[34] D. J. Coffman and D. A. Hegg, *J. Geophys. Res.,* 1995, **100**, 7147.
[35] S. M. Ball, D. R. Hanson, F. L. Eisele and P. H. McMurry, *J. Geophys. Res.,* 1999, **104**, 23709.
[36] A. Paracchino, V. Laporte, K. Sivula, M. Grätzel and E. Thimsen, *Nat. Mater.,* 2011, **10**, 456.
[37] G. Ma, T. Minegishi, D. Yokoyama, J. Kubota and K. Domen, *Chem. Phys. Lett.,* 2011, **501**, 619.
[38] N. Huo, Q. Yue, J. Yang, S. Yang and J. Li, *ChemPhysChem,* 2013, **14**, 4069.
[39] K. Wang, O. Gunawan, T. Todorov, B. Shin, S. J. Chey, N. A. Bojarczuk, D. Mitzi and S. Guha. *Appl. Phys. Lett.,* 2010, **97**, 143508.
[40] S. Yang, Q. Yue, F. Wu, N. Huo, Z. Chen, J. Yang and J. Li, *J. Alloys Compd.*, 2014, **597**, 91.

Keywords

Cu_2ZnSnS_4 nanocrystals, hydrothermal, composites, photocatalysis

Jing Wang, Peng Zhang*, Xuefeng Song, and Lian Gao*

Title

Surfactant-free Hydrothermal Synthesis of Cu_2ZnSnS_4 (CZTS) Nanocrystals and Photocatalytic Properties

ToC figure

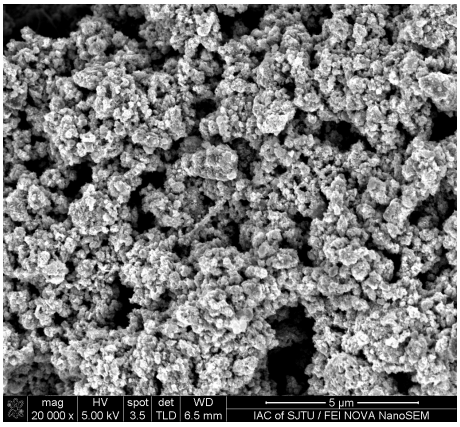

CZTS nanocrystals possessing an average size of 12 nm have been prepared using surfactant-free hydrothermal method and their photocatalytic properties tested both in thin films and in slurry systems.

